Mon. Not. R. Astron. Soc. **372,** 862–868 (2006) doi:10.1111/j.1365-2966.2006.10909.x

Thermal instability in a weakly ionized plasma

H. Stiele,⋆ H. Lesch and F. Heitsch
Universitäts-Sternwarte München (USM), Scheinerstraße 1, 81679 Munich, Germany

Accepted 2006 July 31. Received 2006 July 31; in original form 2006 March 8

ABSTRACT

We revisit the problem of clump formation due to thermal instabilities in a weakly ionized plasma with the help of a linear perturbation analysis, as discussed by Nejad-Asghar & Ghanbari. In the absence of a magnetic field and ambipolar diffusion the characteristic equation reduces to the thermal instability described by Field. We derive the critical wavelengths, which separate the spatial ranges of stability and instability. Contrary to the original analysis of Nejad-Asghar & Ghanbari, perturbations with a wavelength larger than the critical wavelength destabilize the cloud. Moreover, the instability regime of isentropic perturbations is drastically reduced. Isobaric modes with real values of the critical wavelength appear only if the density dependence of the cooling rate is more pronounced than the temperature dependence. Isentropic modes arise only if the power of the density in the cooling rate is smaller than $1/2$, which is not fulfilled for CO cooling. We find that ambipolar diffusion is not a dominating heating process in molecular gas.

Key words: MHD – stars: formation – galaxies: ISM.

1 INTRODUCTION

Star formation is a highly complex process whose details are still not well understood (e.g. Shu, Adams & Lizano 1987; Mac Low & Klessen 2004). There is no doubt, though, that thermal and (magneto-) hydrodynamical instabilities play a crucial role in it.

While gravity certainly is the dominant agent once it comes to actually forming stars (Jeans 1902), the non-linear seeds in molecular clouds necessary for the observed fragmentation (Burkert & Hartmann 2004) might arise from other instabilities. One strong candidate is the thermal instability (Field 1965; Burkert & Lin 2000).

The thermal instability rests on a balance between heating and cooling processes. We choose the atomic interstellar gas and molecular gas, because protostellar cores can only fragment out of their parent clouds, if these are cold and dense enough. The cooling processes are dominated in the atomic interstellar gas by the collisionally excited C II line at 158 μm. In molecular gas the cooling process is dominated by the collisionally excited rotational transition of CO at 2.6 mm ($j = 0 \rightarrow 1$). As long as the gas is optically thin, and barring additional heating processes, the gas would cool catastrophically if it were not for a constant background heating source via cosmic rays and X-rays.

Magnetic fields are omnipresent in the interstellar medium (ISM). Therefore, they must have an influence of the structure and dynamics of interstellar clouds. The ratio of magnetic over resistive time-scales ranges around 10^{15}–10^{21}, so that the field is essentially frozen into the gas. This has led to the notion of magnetic core support, which requires a critical field strength defined by the mass loading of the field line (e.g. Mouschovias & Spitzer 1976). Observations indicate that the field is transcritical, meaning that a good fraction of the cores could well be magnetically supported (e.g. Bourke et al. 2001), although the converse conclusion seems also valid (e.g. Mac Low & Klessen 2004).

Therefore, it is interesting to include magnetic fields to an analysis of thermal instability (see e.g. Nejad-Asghar & Ghanbari 2003, hereafter NAG). In the dense ISM ambipolar drift (Mestel 1985) can lead to a decoupling of ions and neutrals, a mechanism which Shu et al. (1987) made responsible for the control of low-mass star formation. Furthermore, ambipolar drift is associated with a frictional heating rate, which provides an additional heating source in molecular clouds (e.g. Padoan, Zweibel & Nordlund 2000).

We revisit an analysis by NAG, discussing the balance between the thermal instability and ambipolar drift in the context of fragmentation of the molecular gas phase into clumps. We find that – compared to the original analysis – the wavelength dependence of the regions of stability and instability has been inverted. If the wavelength of perturbation is larger than a critical wavelength, the cloud gets unstable. Moreover, the instability regime of isentropic perturbations is drastically reduced.

In Section 2, we use a linear perturbation analysis to find the characteristic equation. The criteria for the domains of stability and instability are derived in Section 3. Including the cooling and heating rates to these criteria, we find critical wavelengths. The requirement of real critical wavelengths leads us to relations between the parameters of the cooling and heating rates (Section 4.1). In Section 4.2, the physical content of these relations is elaborated by applying them to specific cooling rates.

⋆E-mail: stiele@usm.uni-muenchen.de

2 EQUATIONS

We begin with the equations of magnetohydrodynamics (MHD), including ambipolar drift, heat conduction and cooling:

$$\partial_t \rho + \nabla\cdot(\rho \boldsymbol{v}_\mathrm{n}) = 0, \tag{1}$$

$$\rho\,(\partial_t + \boldsymbol{v}_\mathrm{n}\cdot\nabla)\,\boldsymbol{v}_\mathrm{n} + \nabla p + (\nabla\times\boldsymbol{B})\times\boldsymbol{B} = 0, \tag{2}$$

$$\frac{1}{\gamma-1}\,(\partial_t + \boldsymbol{v}_\mathrm{n}\cdot\nabla)\,p - \frac{\gamma}{\gamma-1}\frac{p}{\rho}\,(\partial_t + \boldsymbol{v}_\mathrm{n}\cdot\nabla)\,\rho + \rho\,\Omega - \nabla(K\nabla T) = 0, \tag{3}$$

$$\partial_t \boldsymbol{B} + \nabla\times(\boldsymbol{B}\times\boldsymbol{v}_\mathrm{n}) = \nabla\times\left\{\frac{\boldsymbol{B}}{\gamma_\mathrm{AD}\epsilon\rho^{1+\nu}}\times[\boldsymbol{B}\times(\nabla\times\boldsymbol{B})]\right\}, \tag{4}$$

$$p - \frac{R}{\mu}\rho T = 0. \tag{5}$$

K is the coefficient of thermal conduction, γ is the polytropic index of the ideal gas, μ is the mean atomic mass per particle and R is the universal gas constant.

Equation (4) describes the effect of ambipolar diffusion. γ_AD represents the drag coefficient, which follows from the frictional force between the ions and the neutrals (for details see Shu 1992).

Furthermore, we use the relation $\rho_\mathrm{i} = \epsilon\rho_\mathrm{n}^{\nu}$. This relation represents the fact that in the equilibrium state the recombination rate ($\sim n_\mathrm{i}^2$) equals the ionization rate ($\sim n_\mathrm{n}$). Thus $\rho_\mathrm{i} = \epsilon\rho_\mathrm{n}^{1/2}$. So in the equilibrium state $\nu = 1/2$ is valid. Therefore, $\nu \neq 1/2$ represents a deviation from equilibrium state. Since the ion density is much smaller than the neutral density we approximate $\rho = \rho_\mathrm{i} + \rho_\mathrm{n} \approx \rho_\mathrm{n}$.

The assumption of constant ionization will only be justified if the recombination time-scale is shorter than the cooling time-scale. For hydrogen atoms we can derive the recombination time-scale using the approximation for the recombination coefficient $\alpha^{(2)}$ given by Spitzer (1978):

$$\alpha^{(2)} = \frac{2.06\times10^{-11}\,Z^2}{T^{1/2}}\phi_2(\beta)\,\frac{\mathrm{cm}^3}{\mathrm{s}}, \tag{6}$$

where T denotes the temperature, Z is the nuclear charge and

$$\beta = \frac{158\,000Z^2}{T}. \tag{7}$$

The values for $\phi_2(\beta)$ can be found in table 5.2 of Spitzer (1978). For the temperatures of the cold atomic gas we derive the following expression from that table:

$$\phi_2(\beta) = -152.77\frac{1}{T^{2/3}} + 82.957\frac{1}{T^{1/2}} + 104.537\frac{1}{T} + 1.11. \tag{8}$$

Comparing the recombination time-scales

$$t_\mathrm{rec} = \frac{1}{\alpha^{(2)}\,n} \tag{9}$$

with the cooling time-scales (used density and temperature values can be found in Table 1), we find that the recombination times are more than a magnitude shorter than the cooling times, supporting the assumption of low ionization. In Fig. 1 the dotted lines show the logarithm of the ratio of the recombination time-scale to the cooling time-scale. As both time-scales are proportional to $1/n$ we do not find any density dependence of the ratio.

The net cooling function $\Omega(\rho, T)$ (erg s^{-1} g^{-1}) is defined by

$$\Omega(\rho, T) = \Lambda(\rho, T) - \Gamma_\mathrm{tot}, \tag{10}$$

Table 1. Temperature and density values for the different components of the ISM, used to derive the different time-scales. The values are taken from Ferriére (2001).

Gas	Temperature T (K)	Density n (cm^{-3})
Molecular	10–20	10^2–10^6
Cold atomic	50–100	20–50
Warm atomic	6 000–10 000	0.2–0.5
Warm ionized	∼8 000	0.2–0.5
Hot ionized	$\sim10^6$	∼0.0065

where $\Lambda(\rho, T)$ is the cooling rate given by

$$\Lambda(\rho, T) = \Lambda_0\rho^{\delta}T^{\beta} \tag{11}$$

and Γ_tot is the total heating rate given by

$$\Gamma_\mathrm{tot} = \Gamma_0 + \Gamma_0'\,\rho^{\nu}. \tag{12}$$

In Γ_tot the second term describes a estimation of the heating rate due to ambipolar drift:

$$\Gamma_\mathrm{AD} = \gamma_\mathrm{AD}\epsilon\rho^{\nu}v_\mathrm{d}^2. \tag{13}$$

So $\Gamma_0' \equiv \gamma_\mathrm{AD}\,\epsilon v_\mathrm{d}^2$, where

$$\boldsymbol{v}_\mathrm{d} \equiv \boldsymbol{v}_\mathrm{i} - \boldsymbol{v}_\mathrm{n} = \frac{1}{\gamma_\mathrm{AD}\rho_\mathrm{n}\rho_\mathrm{i}}\,(\nabla\times\boldsymbol{B})\times\boldsymbol{B}. \tag{14}$$

Note that the pressure and gravitational forces on the charged fluid component are negligible compared to the Lorentz force because of the low ionization fraction. Therefore, we assume that the drag force is balanced against the Lorentz force to determine the ion velocity (see equation 14).

Because we are only interested in the effect of ambipolar drift heating, we treat all other contributions to the heating rate as constant, since they depend only weakly on temperature and density e.g. such as photoelectric heating or heating due to cosmic rays and X-rays (see Wolfire et al. 1995).

The cooling rate defines cooling time-scale by

$$t_\mathrm{cool} = \frac{k_\mathrm{B}T}{\mu m_\mathrm{H}\Lambda(\rho, T)}, \tag{15}$$

where m_H is the mass of a hydrogen atom.

Another important time-scale is the local free-fall time-scale which is given by

$$t_\mathrm{ff} = \sqrt{\frac{3\pi}{32G\rho}} \tag{16}$$

with the gravitational constant G.

Comparing these two time-scales we find that for atomic gas the free-fall times are at least three orders of magnitude larger than the cooling times. This is shown by the solid lines in Fig. 1 which give the logarithm of the ratio of the free-fall time-scale to the cooling time-scale. For molecular gas the free-fall times exceed the cooling times by at least five orders of magnitude, as shown by the solid lines of Fig. 2. This time-scale hierarchy means that at the beginning of fragmentation thermal instabilities are more important than gravity (used density and temperature values can be found in Table 1).

For the atomic gas we can achieve a dynamical time-scale by using

$$t_\mathrm{dyn} = \frac{L}{\sqrt{c_\mathrm{s}^2 + a^2}}, \tag{17}$$

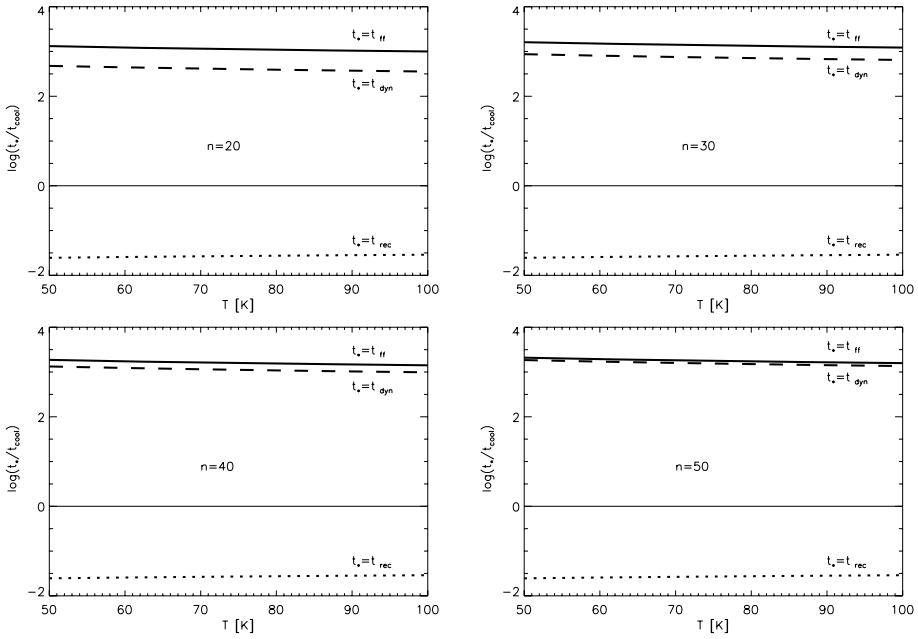

Figure 1. These plots show the logarithm of the ratio of the different time-scales to the cooling time-scale depending on the temperature for different densities ($n = 20, 30, 40, 50$) in the cold atomic gas. The dotted lines belong to the recombination time-scale. The solid and dashed lines correspond to the free-fall and dynamical time-scale, respectively. As the recombination time-scale is more than one order of magnitude shorter than the cooling time-scale the assumption of low ionization is valid. At the beginning of fragmentation thermal instabilities are more important than gravity, due to the fact that the free-fall time-scale exceeds the cooling time-scale by at least three orders of magnitude. The dashed lines show that the cooling time-scale is significantly shorter than the dynamical time-scale.

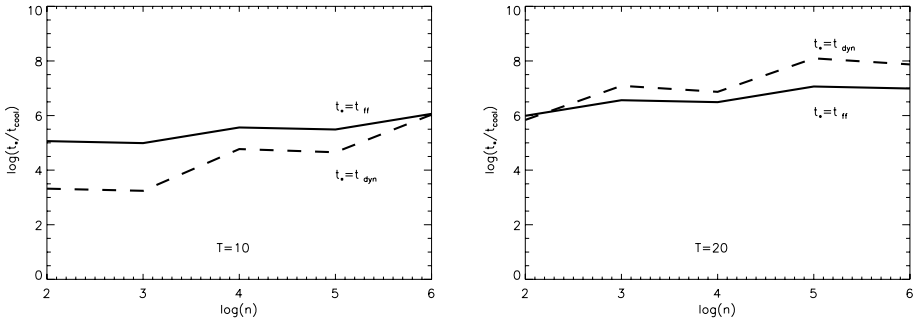

Figure 2. These plots show the logarithm of the ratio of the different time-scales to the cooling time-scale depending on the density for different temperatures ($T = 10, 20$) in molecular clouds. The solid and dashed lines belong to the free-fall and dynamical time-scale, respectively. At the beginning of fragmentation thermal instabilities are more important than gravity, due to the fact that the free-fall time-scale exceeds the cooling time-scale by at least five orders of magnitude. The dashed lines show that the cooling time-scale is significantly shorter than the dynamical time-scale.

where L is the length of the system and a denotes the Alfvén speed. For the molecular gas the velocity can be up to a factor of 10 higher due to turbulent motion. We find from the dashed lines in Figs 1 and 2, which give the logarithm of the ratio of the dynamical time-scale to the cooling time-scale, that for both regimes the cooling time-scale is significantly shorter than the dynamical time-scale.

In the local homogeneous equilibrium state, we have $\rho = \rho_0$, $T = T_0$, $p = p_0$, $\boldsymbol{B} = \boldsymbol{B}_0$, $\boldsymbol{v} = 0$ and $\Omega(\rho_0, T_0) = 0$. Moreover, we set $\boldsymbol{v}_\mathrm{n} \equiv \boldsymbol{v}$. We assume perturbations of the form

$$A(r, t) = A_1 \exp(ht + \mathrm{i}\boldsymbol{k} \cdot \boldsymbol{r}), \tag{18}$$

resulting in a set of linearized equations:

$$h\rho_1 + \mathrm{i}\rho_0(\boldsymbol{k} \cdot \boldsymbol{v}_1) = 0, \tag{19}$$

$$h\rho_0\boldsymbol{v}_1 + \mathrm{i}\boldsymbol{k}p_1 + \mathrm{i}(\boldsymbol{B}_0 \cdot \boldsymbol{B}_1)\boldsymbol{k} - \mathrm{i}(\boldsymbol{k} \cdot \boldsymbol{B}_0)\boldsymbol{B}_1 = 0, \tag{20}$$

$$\frac{h}{\gamma - 1}p_1 - \frac{h\gamma}{\gamma - 1}\frac{p_0}{\rho_0}\rho_1 + \rho_0\Omega_\rho\rho_1 + \rho_0\Omega_T T_1 + Kk^2T_1 = 0, \tag{21}$$

$$h\boldsymbol{B}_1 + \mathrm{i}\boldsymbol{B}_0(\boldsymbol{k} \cdot \boldsymbol{v}_1) - \mathrm{i}(\boldsymbol{k} \cdot \boldsymbol{B}_0)\,\boldsymbol{v}_1 = \mathrm{i}\boldsymbol{k} \times \left\{ \frac{\boldsymbol{B}_0}{\gamma_\mathrm{AD}\epsilon\rho_0^{1+\nu}} \times [\boldsymbol{B}_0 \times (\mathrm{i}\boldsymbol{k} \times \boldsymbol{B}_1)] \right\}, \tag{22}$$

$$\frac{p_1}{p_0} - \frac{\rho_1}{\rho_0} - \frac{T_1}{T_0} = 0, \tag{23}$$

where $\Omega_\rho \equiv (\partial\Omega/\partial\rho)_T$ and $\Omega_T \equiv (\partial\Omega/\partial T)_\rho$ are evaluated for the equilibrium state.

We introduce a coordinate system with the following unit vectors:

$$\hat{\boldsymbol{e}}_z = \frac{\boldsymbol{B}_0}{B_0}, \quad \hat{\boldsymbol{e}}_y = \frac{\boldsymbol{B}_0 \times \boldsymbol{k}}{|\boldsymbol{B}_0 \times \boldsymbol{k}|}, \quad \hat{\boldsymbol{e}}_x = \hat{\boldsymbol{e}}_y \times \hat{\boldsymbol{e}}_z. \tag{24}$$

The set of equations splits into two subsystems, one depending only on the y direction and one depending on x and z directions.

The system depending on y describes disturbances perpendicular to the $(\boldsymbol{B}_0, \boldsymbol{k})$ plane:

$$h\rho_0 v_{1y} - \mathrm{i}k_z B_0 B_{1y} = 0, \tag{25}$$

$$-\mathrm{i}k_z B_0 v_{1y} + \left(h + \frac{B_0^2 k_z^2}{\gamma_{\mathrm{AD}}\epsilon\rho_0^{1+\nu}}\right) B_{1y} = 0. \tag{26}$$

They have a solution of the form

$$h_{1,2} = -\frac{(ak_z)^2}{2\gamma_{\mathrm{AD}}\epsilon\rho_0^{\nu}} \pm \mathrm{i}k_z a\sqrt{1 - \left(\frac{k_z a}{2\gamma_{\mathrm{AD}}\epsilon\rho_0^{\nu}}\right)^2} \tag{27}$$

with $a \equiv (B_0/\sqrt{\rho_0})$ the Alfvén speed.

As the real part of these solutions is negative, the system is stable. Therefore, we are not interested in these solutions.

For the system in the x, z plane we introduce some 'shortcuts':

$$k_z^2 = k^2\cos^2\theta, \quad h' = \frac{k^2 a^2}{\gamma_{\mathrm{AD}}\epsilon\rho_0^{\nu}}, \quad c_{\mathrm{s}} = \sqrt{\gamma\frac{p_0}{\rho_0}}, \tag{28}$$

$$k_\rho = \frac{\mu(\gamma-1)\rho_0\Omega_\rho}{Rc_{\mathrm{s}}T_0},\ k_T = \frac{\mu(\gamma-1)\Omega_T}{Rc_{\mathrm{s}}} + \frac{\mu(\gamma-1)K}{Rc_{\mathrm{s}}\rho_0}k^2 \tag{29}$$

and a few dimensionless quantities:

$$y \equiv \frac{h}{kc_{\mathrm{s}}},\ \sigma_\rho \equiv \frac{k_\rho}{k},\ \sigma_T \equiv \frac{k_T}{k},\ \alpha = \left(\frac{a}{c_{\mathrm{s}}}\right)^2,\ D \equiv \frac{h'}{kc_{\mathrm{s}}} \tag{30}$$

and find the following characteristic equation:

$$\begin{aligned} y^5 &+ y^4(\sigma_T + D) + y^3(1 + \alpha + \sigma_T D) \\ &+ y^2\left[\gamma^{-1}(\sigma_T - \sigma_\rho) + \alpha\sigma_T + D\right] \\ &+ y\left[\alpha\cos^2\theta + \gamma^{-1}(\sigma_T - \sigma_\rho)D\right] \\ &+ \gamma^{-1}\alpha(\sigma_T - \sigma_\rho)\cos^2\theta = 0, \end{aligned} \tag{31}$$

where θ is the angle between the direction of propagation of the perturbations and the magnetic field lines, α describes the ratio of the Alfvén speed to the sound speed (c_{s}), the reciprocal of h' corresponds to the time-scale of ambipolar diffusion and thus D represents the ratio of h' to the angular frequency of a perturbation propagating with the sound speed. $\sigma_\rho(k_\rho)$ and $\sigma_T(k_T)$ depend on the density and temperature derivative of the net cooling function, respectively, whereas $\sigma_T(k_T)$ also depend on the thermal conduction. y denotes the dimensionless angular frequency, which we are interested in.

3 REGIONS OF STABILITY AND INSTABILITY

To separate the regions of stability (all $\Re(y) < 0$) and instability (at least one $\Re(y) > 0$), we investigate the change of the sign of the roots, depending on the parameters σ_ρ and σ_T, knowing the values of α, D and θ. The situation for a negligible magnetic field is shown in Fig. 3 and for a non-negligible magnetic field there are some examples given in Fig. 4.

For $\sigma_\rho > 0$ the change of the sign does not depend on the values of α, D and θ and can be described by

$$\sigma_\rho = \sigma_T. \tag{32}$$

For $\sigma_\rho < 0$ and $\theta = 0$ the change of the sign does not depend on the values of α and D and we can describe it by

$$\sigma_T + \frac{3}{2}\sigma_\rho = 0. \tag{33}$$

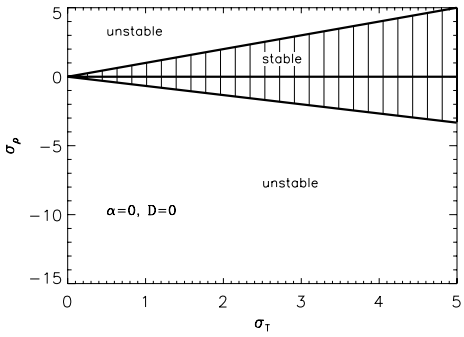

Figure 3. Regions of stability and instability, in the case of a negligible magnetic field. The abscissa is the normalized form of the temperature derivative of Ω, as modified by thermal conduction in equations (29 and 30) and the ordinate is related to the density derivative of Ω. In the shaded area the system is stable, whereas the unshaded areas represent the regions of instability. The changes due to a non-negligible magnetic field are shown in Fig. 4.

If $\theta \neq 0$ the change of the sign does depend on the values of α and D. This leads to regions of semistability.

Semistable indicates that the exact shape of the curve which describes the change between the region of stability and instability depends on θ, the angle between the direction of propagation of the perturbations and the magnetic field lines.

Fig. 4 should be compared to fig. 2 of NAG. Note that from equations (29) and (30), we find that σ_T can only be negative if $\Omega_T < 0$. As the chosen heating rate does not depend on the temperature, Ω_T can only be negative if $\mathrm{d}(\Lambda_0\rho^\delta T^\beta)/\mathrm{d}T < 0$. This is only possible if β is negative, which contradicts the behaviour of the cooling functions. Thus $\sigma_T > 0$.

With the net cooling function equation (10), we get for σ_ρ:

$$\sigma_\rho = \frac{\mu(\gamma-1)}{kRc_{\mathrm{s}}T_0}\Lambda(\rho_0, T_0)(\delta - \nu\xi) \tag{34}$$

with

$$\xi = \frac{\Gamma_0'\rho_0^{\nu}}{\Lambda(\rho_0, T_0)}. \tag{35}$$

Note that equation (35) is the inverse of the expression given by NAG, equation (25).

Similarly, σ_T can be derived as

$$\sigma_T = \frac{\mu(\gamma-1)}{kRc_{\mathrm{s}}T_0}\beta\Lambda(\rho_0, T_0)\left[1 + \left(\frac{\lambda_0}{\lambda}\right)^2\right] \tag{36}$$

with $\lambda_0 = 2\pi\sqrt{(KT_0)/(\rho_0\beta\Lambda(\rho_0, T_0))}$ and $k = (2\pi/\lambda)$.

This expression is derived from equation (29) and (30), so that $\sigma_T > 0 \forall\lambda$. Due to a sign error NAG arrive at a different conclusion, namely that the final factor of equation (36) is $[1 - (\lambda_0/\lambda)^2]$ (Nejad-Asghar and Ghanbari, private communication).

Since $\sigma_T > 0\,\forall\lambda$, the behaviour of the system will depend on the sign of σ_ρ. From the definition of σ_ρ (equation 34) we find that the sign is defined by $\delta - \nu\xi$. The behaviour of that expression will be discussed in the next section.

For $k_\rho > 0$ follows $\delta > \xi\nu$ and thus (equation 32)

$$\sigma_\rho = \sigma_T.$$

With equations (34) and (36) we find a critical wavelength of

$$\lambda_{\mathrm{c1}} = \frac{\lambda_0}{\sqrt{(\delta - \nu\xi)/(\beta) - 1}}. \tag{37}$$

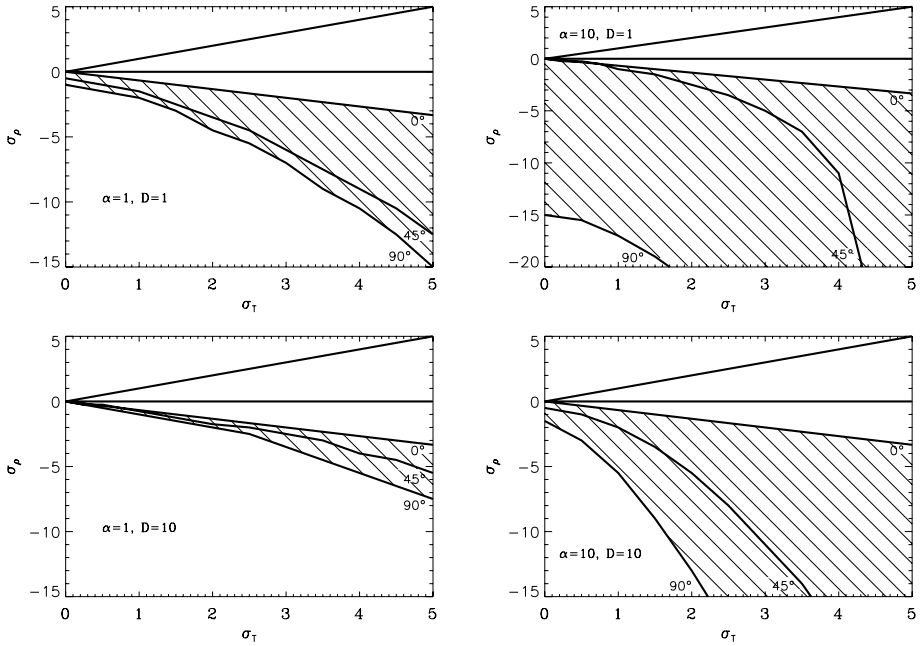

Figure 4. Regions of stability and instability. The shaded areas are semistable regions, where the exact shape of the curve which describes the change between the region of stability and instability depends on θ, the angle between the direction of propagation of the perturbations and the magnetic field lines. For $\sigma_\rho > 0$ there are only isobaric instabilities possible, whereas for $\sigma_\rho < 0$ there occur only isentropic instabilities.

Compared to the result of NAG the sign of the summands in the square root are reversed, meaning that real critical wavelengths of NAG will get imaginary and vice versa. Furthermore, the wavelength dependence of the stability relation is inverted: if the wavelength of the perturbation is larger than the critical wavelength (equation 37), there will occur isobaric instabilities. Otherwise the system is stable (see equation 44).

For the case $k_\rho < 0$, i.e. $\delta < \xi\nu$, we get (equation 33)

$$\sigma_T + \frac{3}{2}\sigma_\rho = 0,$$

and again with equations (34) and (36) we arrive at a critical wavelength

$$\lambda_{c2} = \frac{\lambda_0}{\sqrt{(3/2\,(\nu\xi - \delta))/(\beta) - 1}}. \tag{38}$$

Compared to λ_{c3} of NAG (equation 28 of NAG) the sign of the summands in the square root are reversed. Again the wavelength dependence is inverted. This time a wavelength larger than the critical one allows isentropic perturbations. For $\lambda < \lambda_{c2}$ the system stays stable (see equation 45).

As discussed previously it is not possible to reach $\sigma_T < 0$ for chosen cooling and heating rates. Therefore, it cannot be used to derive a critical wavelength. Anyhow NAG derived a critical wavelength and called it λ_{c2}, but it also suffers from the sign error in equation (36).

The behaviour of the isobaric mode can be gleaned from rewriting σ_ρ and σ_T and assuming that the wavelength is a multiple of the critical wavelength: $\lambda = b\lambda_{c1}$.

$$\sigma_\rho = \frac{\mu(\gamma-1)}{2\pi R c_s T_0}\Lambda(\rho_0, T_0)\,(\delta - \nu\xi)\,b\lambda_{c1}, \tag{39}$$

$$\sigma_T = \frac{\mu(\gamma-1)}{2\pi R c_s T_0}\beta\Lambda(\rho_0, T_0) b\lambda_{c1}\left[1 + \left(\frac{\lambda_0}{b\lambda_{c1}}\right)^2\right], \tag{40}$$

$$\sigma_T = \frac{\mu(\gamma-1)}{2\pi R c_s T_0}\beta\Lambda(\rho_0, T_0) b\lambda_{c1}\left[1 + \left(\frac{\lambda_0}{\lambda_{c1}}\right)^2\right] - \frac{\mu(\gamma-1)}{2\pi R c_s T_0}\beta\Lambda(\rho_0, T_0)\frac{b^2-1}{b}\frac{\lambda_0^2}{\lambda_{c1}}. \tag{41}$$

Thus,

$$\sigma_\rho = b\sigma_{\rho\,c}, \tag{42}$$

$$\sigma_T = b\sigma_{T\,c} + \Delta\sigma_T. \tag{43}$$

For $b > 1$, i.e. $\lambda > \lambda_{c1} \Rightarrow (b^2-1)/(b) > 0 \Rightarrow \Delta\sigma_T < 0$

$$\Rightarrow \text{ unstable.} \tag{44}$$

For $b < 1$, i.e. $\lambda < \lambda_{c1} \Rightarrow (b^2-1)/(b) < 0 \Rightarrow \Delta\sigma_T > 0$
$\Rightarrow$ stable.
For the isentropic mode we find the same behaviour.
For $b > 1$, i.e. $\lambda > \lambda_{c2} \Rightarrow (b^2-1)/(b) > 0 \Rightarrow \Delta\sigma_T < 0$

$$\Rightarrow \text{ semistable.} \tag{45}$$

For $b < 1$, i.e. $\lambda < \lambda_{c2} \Rightarrow (b^2-1)/(b) < 0 \Rightarrow \Delta\sigma_T > 0$
$\Rightarrow$ stable.

If we take a wavelength, which is a factor b of the critical wavelength for the isobaric mode (λ_{c1}), we find that σ_ρ and σ_T changes proportional to the factor b (see equation 42 and the first summand of equation 43). If this were correct the system would evolve along the line which separates the region of stability from the region of instability, when b changes. But in addition σ_T has a second summand (see equation 43). Therefore, $(b^2-1)/b$ determines the stability of the system with wavelength $\lambda = b\lambda_{c1}$. For $b > 1$, $(b^2-1)/b$ is positive. From the definition of the additional term in σ_T, called $\Delta\sigma_T$, it follows that $\Delta\sigma_T$ has to be negative. This means that σ_T gets smaller than in the critical case and that therefore we find the new σ_T on the left-hand side of the separation line, where the system is unstable.

For $b < 1$, $(b^2 - 1)/b$ is negative and therefore $\Delta\sigma_T$ is positive. Now σ_T is bigger than in the critical case and hence the system is stable. This is expressed in a short way in equation (44).

For the isentropic mode we repeat this analysis. Now we take a wavelength, which is a factor b of the critical wavelength for isentropic perturbations, called λ_{c2}. We find again that σ_ρ and σ_T show a behaviour proportional to b, and that σ_T has again an additional term, which shows the same b dependence as before. For $b > 1$, $(b^2 - 1)/b$ is positive and hence $\Delta\sigma_T < 0$. This means that σ_T gets smaller than in the critical case and that therefore we find the new σ_T on the left-hand side of the separation line, where the system is semistable. For $b < 1$, $(b^2 - 1)/b$ is negative and hence $\Delta\sigma_T > 0$. This time σ_T is bigger than in the critical case and the system remains stable. The short version can be found in equation (45).

Summarizing, instability can only occur for $\lambda > \lambda_c$. Although not included explicitly in our analysis, an upper length scale limit for the instability is set by the condition that the sound crossing time be smaller than the cooling time (see e.g. Burkert & Lin 2000).

4 PHYSICAL INTERPRETATION

4.1 Relations between the parameters of cooling and heating rates

For negligible thermal conduction ($K = 0$), the critical wavelengths equations (37) and (38) are zero. This means that independent of the scale of the perturbation there will always be a collapsing mode.

To find regions of stability and instability we have to assume a non-vanishing thermal conduction. We begin with the isobaric criterion. For $\lambda_c \in |\mathrm{R}|$,

$$\frac{\delta - \nu\xi}{\beta} > 1 \tag{46}$$

is required. As δ and β depend on the cooling function and $\nu = 1/2$ in the equilibrium state, the only free parameter is ξ. We find that

$$\xi < \frac{\delta - \beta}{\nu}. \tag{47}$$

From equation (35) follows that $0 < \xi < 1$, where the extremes correspond to the cases no heating due to ambipolar diffusion ($\xi = 0$) and only heating due to ambipolar diffusion ($\xi = 1$). Hence, the density dependence of the cooling function must be stronger than the temperature dependence, i.e.

$$\delta > \beta. \tag{48}$$

As in the equilibrium state $\Lambda(\rho_0, T_0) = \Gamma_0 + \Gamma_{\mathrm{AD}}$ we find that

$$\Gamma_0 = \Gamma_{\mathrm{AD}} \left(\frac{1}{\xi} - 1 \right). \tag{49}$$

Isentropic modes could occur, if $\delta < \xi\nu$. This requires that

$$\delta < 1/2. \tag{50}$$

Then we find that

$$\xi > \frac{(2/3)\beta + \delta}{\nu}, \tag{51}$$

where $\xi < 1$ still holds.

4.2 Application to cooling rates

For the cold atomic gas C II represents the most important coolant, because it has transitions which lie in the temperature range of atomic gas, because this ion is highly abundant, and the relative ease of collisional excitation (see Pottasch, Wesselius & van Duinen 1979; Gry, Lequeux & Boulanger 1992; Wolfire et al. 1995). An expression for this cooling rate is given by Spitzer (1978):

$$\rho\Lambda_{\mathrm{CII}} = 7.9 \times 10^{-27} \exp\left(\frac{-92}{T}\right) n^2 \,\mathrm{erg\,cm^{-3}\,s^{-1}}. \tag{52}$$

Since in our formalism we have to write the cooling function as $\Lambda = \Lambda_0 \rho^\delta T^\beta$, we parametrize equation (52) for $T < 500\,\mathrm{K}$ as

$$\Lambda_{\mathrm{CII}} = \frac{7.9 \times 10^{-27}}{\mu^2 m_{\mathrm{H}}^2} 2.2 \times 10^{-2} T^{0.60} \rho \frac{\mathrm{erg}}{\mathrm{g\,s}}. \tag{53}$$

Thus $\delta = 1$ and $\beta = 0.6$. It should be remarked that owing to the nature of the exponential and power function, we only get a very rough estimate. The approximation shows deviations of 20–40 per cent from equation (52). Depending on the chosen temperature range the value of β can differ considerably ($0.2 \leqslant \beta < 1.1$). As $\delta > 0.5$ (see equation 50) we can only expect isobaric instabilities. Because $\delta > \beta$ (see equation 48) we can calculate ξ as $\xi < 0.8$. Thus we find that $\Gamma_0 > 0.25\,\Gamma_{\mathrm{AD}}$. Taking $K = 2.8 \times 10^2\,\mathrm{erg\,cm^{-1}\,s^{-1}\,K^{-1}}$ (see Vazquenz-Semadeni et al. 2003) we achieve critical wavelengths of a few thousandth parsec, above which the system will be unstable.

For molecular gas CO is the most important coolant, because it has a rotational transition and is the second frequent molecule in the ISM. We take the CO cooling rate ($j = 0 \rightarrow 1$, excitation due to collisions with hydrogen atoms) given by Dalgarno & McCray (1972):

$$\rho\Lambda_{\mathrm{CO}} = 7.5 \times 10^{-27} T^{1/2} \exp(-5.3/T)\, n^2 \frac{\mathrm{erg}}{\mathrm{cm^3\,s}} \tag{54}$$

and rewrite it as ($10 \leqslant T < 50$)

$$\Lambda_{\mathrm{CO}} = \frac{7.5 \times 10^{-27}}{\mu^2 m_{\mathrm{H}}^2} 3.3 \times 10^{-1} T^{0.76} \rho \frac{\mathrm{erg}}{\mathrm{g\,s}}. \tag{55}$$

This means that $\delta = 1$ and $\beta = 0.76$. As again $\delta > 0.5$ (see equation 50) the modes can only be isobaric. Calculating ξ we get that $\xi < 0.48$. This means that heating due to ambipolar diffusion only provides a contribution to the total heat input into the molecular cloud. Taking $\Gamma_0 > 1.08\Gamma_{\mathrm{AD}}$ and $K = 2.8 \times 10^2\,\mathrm{erg\,cm^{-1}\,s^{-1}\,K^{-1}}$ we achieve again critical wavelengths of a few thousandth parsec.

Another CO cooling rate (excitation due to collisions with He atoms and H_2 molecules), given as a plot, can be found in Gilden (1984). With a two-dimensional fit we can write it as

$$\Lambda_{\mathrm{CO}} = \frac{2.3 \times 10^{-25}}{\mu^{1.58} m_{\mathrm{H}}^{1.58}} T^{0.77} \rho^{0.58} \frac{\mathrm{erg}}{\mathrm{g\,s}}. \tag{56}$$

This time $\delta = 0.58$ and $\beta = 0.77$. As $\delta > 0.5$ we expect isobaric modes, but get an imaginary critical wavelength, because $\beta > \delta$.

The results are summarized in Fig. 5.

5 SUMMARY

In this paper we have examined the conditions for clump formation due to thermal instabilities in the presence of a magnetic field.

Comparing the cooling time-scales to the dynamical time-scales and local free-fall time-scales, we found that the first of these is clearly shorter (at least two orders of magnitude) than either of the other two. This suggests that the gas will lose all memory of any structure imposed by the cooling instability during its subsequent turbulent collapse.

A linear perturbation analysis of the MHD equations including ambipolar drift yields the characteristic equation, following NAG. Neglecting the effects of the magnetic field, we retrieved the prior

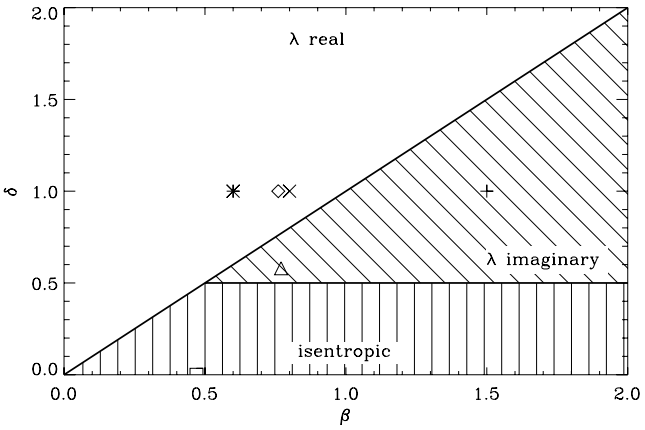

Figure 5. Isobaric instability regimes in terms of temperature dependence β and density dependence δ. The isentropic mode is shaded vertically. $*$ represents C II cooling. $\Diamond$ (Dalgarno & McCray) and $\triangle$ (Gilden) stand for CO cooling. $+$ denotes CH cooling, $\times$ Si II cooling and $\square$ H_2 cooling. In the cases $*$, x and $\Diamond$ the critical wavelength is real, meaning that only in this regime physical conclusions are possible. Whereas in cases $\triangle$ and $+$ it is imaginary. This shows the limitation of the method used. Because of the linearization of the cooling and heating rates it can only be applied to specific cooling rates. In the case of H_2 cooling ($\square$) we have isentropic perturbations.

results of the linear thermal instability (Field 1965). From the investigation of the sign of the roots we isolated conditions to distinguish between regions of stability and instability. Inserting a parametrized cooling rate and heating due to ambipolar diffusion in these expressions, we derived critical wavelengths λ_c. Requiring real critical wavelengths ($\lambda_c \in |R|$) led to relations between the parameters of the cooling and heating rates. To elaborate the physical content of these relations we applied them to specific cooling rates.

Comparing to the analysis of NAG we found that the wavelength dependence of the regions of stability and instability has been inverted. If the wavelength of perturbation is larger than the critical wavelength the cloud gets unstable. In the case of isentropic perturbations we still find a region of semistability, where thermal instability allows compression along the local magnetic field lines but not perpendicular to it. However, the parameter space for semistability and instability is reduced, because for the chosen heating and cooling rates it is not possible to reach a negative temperature derivative of the net cooling function (i.e. $\sigma_T < 0$).

Molecular clouds with negligible thermal conduction will always collapse, independent from the length scale of the perturbation. The upper length scale for instability is set by the sound crossing time (e.g. Burkert & Lin 2000). To simplify our analysis we have neglected the effect of self-gravity. Taking it into account must be the aim of a subsequent investigation. We would expect that self-gravity contributes to fragmentation and accelerates clump formation in molecular clouds.

Including thermal conduction isobaric modes can only occur if the density dependence of the cooling rate is more pronounced than the temperature dependence. We have found also that in molecular clouds heating due to ambipolar diffusion only provides a contribution to the total heating rate, which is at maximum 48 per cent of the cooling rate. To reach an equilibrium state on which the analysis is based, there must be other heating rates which are at least as important as heating due to ambipolar diffusion e.g. heating due to cosmic rays and X-rays, reconnection heating or photoelectric heating on grain surface. They should provide more than 50 per cent to the heating rate. To get isentropic modes the power of the density in the cooling rate $\delta < 1/2$, which is not fulfilled for CO cooling, the most important cooling for molecular clouds.

In the context of our thermal instability analysis, we find only a weak influence of the magnetic field on the stability of the molecular cloud.

ACKNOWLEDGMENT

We thank the referee for the critical and very constructive report.

REFERENCES

Bourke T. L., Myers P. C., Robinson G., Hyland A. R., 2001, ApJ, 554, 916
Burkert A., Hartmann L., 2004, ApJ, 616, 288
Burkert A., Lin D. N. C., 2000, ApJ, 537, 270
Dalgarno A., McCray R. A., 1972, ARA&A, 10, 375
Ferriére K. M., 2001, Rev. Mod. Phys., 73, 1031
Field G. B., 1965, ApJ, 142, 531
Gilden D. L., 1984, ApJ, 279, 335
Gry C., Lequeux J., Boulanger F., 1992, A&A, 266, 457
Jeans Sir J. H., 1902, Phil. Trans. R. Soc. Lond., 199, 1
Mac Low M.-M., Klessen R., 2004, Rev. Mod. Phys., 76, 125
Mestel L., 1985, in Black D. C., Matthews M. S., eds, Protostars and Planets II. Univ. Arizona Press, Tucson, p. 320
Mouschovias T. Ch., Spitzer L., Jr, 1976, ApJ, 210, 326
Nejad-Asghar M., Ghanbari J., 2003, MNRAS, 345, 1323 (NAG)
Padoan P., Zweibel E., Nordlund Å., 2000, ApJ, 540, 332
Pottasch S. R., Wesselius P. R., van Duinen R. J., 1979, A&A, 74, 15
Shu F., 1992, The Physics of Astrophysics, Vol. II, Gas Dynamics. University Science Books, Mill Valley, CA
Shu F. H., Adams F. C., Lizano S., 1987, ARA&A, 25, 23
Spitzer L., 1978, Physical Processes in the Interstellar Medium. John Wiley & Sons, New York
Vazquez-Semadeni E., Gaziol A., Passot T., Sanchez-Salcedo J., 2003, Lect. Notes Phys., 614, 213
Wolfire M. G., Hollenbach D., McKee C. F., Tielens A. G. G. M., Bakes E. L. O., 1995, ApJ, 443, 152

This paper has been typeset from a TEX/LATEX file prepared by the author.